



# GIS dataset: geomorphological record of terrestrial-terminating ice streams, southern sector of Baltic Ice Stream Complex, last Scandinavian Ice Sheet, Poland

Izabela Szuman<sup>1</sup>, Jakub Z. Kalita<sup>1</sup>, Marek W. Ewertowski<sup>1</sup>, Chris D. Clark<sup>2</sup>, Stephen J. Livingstone<sup>2</sup>,  
5 Leszek Kasprzak<sup>1</sup>

<sup>1</sup>Faculty of Geographical and Geological Sciences, Adam Mickiewicz University, Poznań, 61-680, Poland

<sup>2</sup>Department of Geography, University of Sheffield, Sheffield, S3 7ND, UK

Correspondence to: Izabela Szuman (szuman@amu.edu.pl)

**Abstract.** Here we present a comprehensive dataset of glacial geomorphological features covering an area of 65 000 km<sup>2</sup> in  
10 central west Poland, located along the southern sector of the last Scandinavian Ice Sheet, within the limits of the Baltic Ice  
Stream Complex. The GIS dataset is based on mapping from a 0.4 m high-resolution Digital Elevation Model derived from  
airborne Light Detection and Ranging data. Ten landform types have been mapped: Mega-Scale Glacial Lineations,  
drumlins, marginal features (moraine chains, abrupt margins, edges of ice-contact fans), ribbed moraines, tunnel valleys,  
eskers, geometrical ridge networks and hill-hole pairs. The map comprises 5461 individual landforms or landform parts,  
15 which are available as vector layers in GeoPackage format at <http://doi.org/10.5281/zenodo.4570570> (Szuman et al., 2021a).  
These features constitute a valuable data source for reconstructing and modelling the last Scandinavian Ice Sheet extent and  
dynamics from the Middle Weichselian Scandinavian Ice Sheet advance, 50 – 30 ka BP, through the Last Glacial Maximum,  
25 – 21 ka BP and Young Baltic Advances, 18 – 15 ka BP. The presented data are particularly useful for modellers,  
geomorphologists and glaciologists.

## 20 1 Introduction

Present-day ice sheet mass loss is a key driver of global average sea-level rise (Rignot et al., 2019). A key challenge is to  
quantify the sensitivity of ice sheets to climate change to improve future predictions of ice sheet mass loss and sea level rise.  
However, the observational time scale for contemporary ice sheets is short (decades) and it is a challenge to access their  
beds, contrary to the footprint of their palaeo-analogues (Stokes and Clark, 2001). Reconstructions of the configuration and  
25 evolution of palaeo-ice sheets through glacial cycles therefore provide a critical long-term constraint for testing and  
calibrating ice sheet models (e.g. Hughes, 2009; Stokes et al., 2015 and the references therein; Patton et al., 2016a; Patton et  
al., 2017; Ely et al., 2019a).

Geomorphological mapping is a powerful tool for reconstructing the glacial history of formerly glaciated areas (Clark,  
1997; Kleman et al., 1997; Kjær et al., 2003), especially where *in situ* dating results (e.g., OSL, cosmogenic nuclides dating,



30 C14) are too sparse to reproduce highly dynamic ice sheet behaviour. Additionally, geomorphological mapping is widely  
used for shedding light on glacial processes, the evolution of landforms and for reconstructing ice sheets dynamics (e.g.  
Lukas, 2006;Kleman et al., 2008;Ó Cofaigh et al., 2008;Hughes, 2009;King et al., 2009;Kleman et al., 2010;Spagnolo et al.,  
2014;Ely et al., 2016;Evans et al., 2016;Jamieson et al., 2016;Chandler et al., 2018). A difficulty in acquiring accurate  
35 information on glacial landforms lies in the degradation of their original forms by postglacial processes, including water  
erosion, aeolian activity, permafrost, or slope processes and human activity (Spagnolo et al., 2014). The results of ice sheet  
modelling are increasingly compared with or improved by incorporating geomorphological and geological field data (Stokes  
and Tarasov, 2010;Patton et al., 2017) and tools have been developed to aid such comparisons (e.g. Napieralski et al.,  
2006;Napieralski et al., 2007;Ely et al., 2019b).

The widespread presence of cross-cutting lineations has enabled reconstructions of the last Scandinavian Ice Sheet's (SIS)  
40 growth and decay, relative switches in ice flow and the identification of ice streams (Kleman et al., 1997;Punkari,  
1997;Boulton et al., 2001). The Baltic Ice Stream Complex (BISC) was one of the most prominent of the SIS ice streams.  
Typically, results from empirical and numerically modelled reconstructions (Kleman et al., 1997;Punkari, 1997;Houmark-  
Nielsen, 2010;Patton et al., 2016a;Patton et al., 2017) show the BISC as a vast area of highly dynamic, fast-flowing ice  
discharging towards the southern margin in northern Europe. However, there is lack of empirical data constraining the  
45 southern margin of the BISC that can lead to ambiguities in understanding its behavior, which has resulted in millennial  
scale time differences between alternate reconstructions (cf. Hughes et al., 2016;Stroeven et al., 2016).

The specific role of ice streams in ice sheet mass balance is somewhat controversial. They are responsible for ~90% of the  
discharge of the Antarctic Ice Sheet (Bamber et al., 2000) with Pine Island and Thwaites ice streams contributing 32% of the  
discharge (Bamber and Dawson, 2020). Dynamic variations such as ice stream slowdown or stagnation can lead to a positive  
50 mass balance (Joughin and Tulaczyk, 2002); for example, the Kamb Ice Stream stagnated about 150 years ago (Retzlaff and  
Bentley, 1993). Flow instabilities within ice sheets can lead to rapid ice discharges, with the Hudson Strait Ice Stream of the  
Laurentide Ice Sheet, for example, undergoing catastrophic purge events of accelerated ice discharge in response to positive  
basal thermal conditions, which led to increased meltwater production and thawing of soft subglacial sediments (MacAyeal,  
1993;Rahmstorf, 2002). When considered across wider temporal and spatial scales ice streams can be thought of as drainage  
55 networks, and for the Laurentide Ice Sheet these networks have been shown to scale fairly predictably with ice sheet volume  
(Stokes et al., 2016).

In this paper we use a new high-resolution digital elevation model to produce a comprehensive, high-quality geospatial  
dataset containing updated and newly discovered glacial landforms along the Polish southern sector of the SIS. These data  
can be used to reconstruct basal conditions, the pattern and style of retreat and ice flow dynamics during previous  
60 glaciations. This area is of particular interest as it was at the southernmost limit of the BISC, which was highly active during  
the last glaciation and a key control governing SIS drainage and collapse (Patton et al., 2017).



## 2 Study area

The southern sector of the SIS was drained by the so-called BISC (Boulton et al., 2001, 2004;Kalm, 2012), which comprised several branches of fast flowing ice across the central European plains (see Punkari, 1997;Boulton et al., 2001;Stokes and Clark, 2001). The region of central west Poland was glaciated: (1) during the Middle Weichselian c. 30 - 50 ka BP (Wysota et al., 2009 and the references therein;Houmark-Nielsen, 2010;Hughes et al., 2016); (2) the Late Weichselian local Last Glacial Maximum (LGM), that took place between 25 and 21 ka BP (Tylmann et al., 2019); and (3) partly during two Young Baltic advances after 18 ka BP (Kjær et al., 2003;Stroeven et al., 2016). The southernmost position of the SIS margin, in central west Poland, was slightly south of 52°N (Fig. 1) and was attained during the local LGM (Leszno/Brandenburg Phase). The Young Baltic advances are shown to be correlated with the Poznań/Frankfurt Phase and the Pomeranian Phase (Stroeven et al., 2016). The retreat of the ice sheet northwards across the Baltic Sea occurred at about 16.5 ka (Stroeven et al., 2016).

The study area covers c. 65 000 km<sup>2</sup> of central west Poland. This region was occupied by ice streams flowing from the north west (from Lower Odra region – LOR) and north east (Lower Wisła region – LWR) (Fig. 1). The earliest studies focused on glacial landform mapping across the study area were based on geomorphological field mapping by the Prussian Geological Survey at the end of the 19<sup>th</sup> and beginning of the 20<sup>th</sup> centuries (e.g. Berendt and Keilhack, 1894;Korn, 1912;Assmann and Dammer, 1916;Woldstedt, 1935). Further studies comprised geomorphological field mapping and analogue topographic maps analysis (Krygowski, 1947;Kozarski, 1959;Galon, 1961;Bartkowski, 1962;Kozarski, 1962;Bartkowski, 1963;Karczewski, 1963;Krygowski, 1963;Bartkowski, 1964, 1967, 1968;Stankowski, 1968;Bartkowski, 1969;Karczewski, 1971;Bartkowski, 1972;Kozarski, 1978;Karczewski et al., 1980;Liedtke, 1981;Rotnicki and Borówka, 1989, 1994;Kozarski, 1995). The first remote mapping attempts were based on Digital Elevation Models (DEM) with a resolution of 30 m and topographic maps with scales of 1:50000 and 1:10000 (Ewertowski and Rzeszewski, 2006;Przybylski, 2008). Streamlined bedforms along Stargard Drumlin Field, in the north western portion of the study area, along the LOR, were investigated by Keilhack (1897), Karczewski (1976) and more recently, by Hermanowski et al. (2019) (see Fig. 1B).

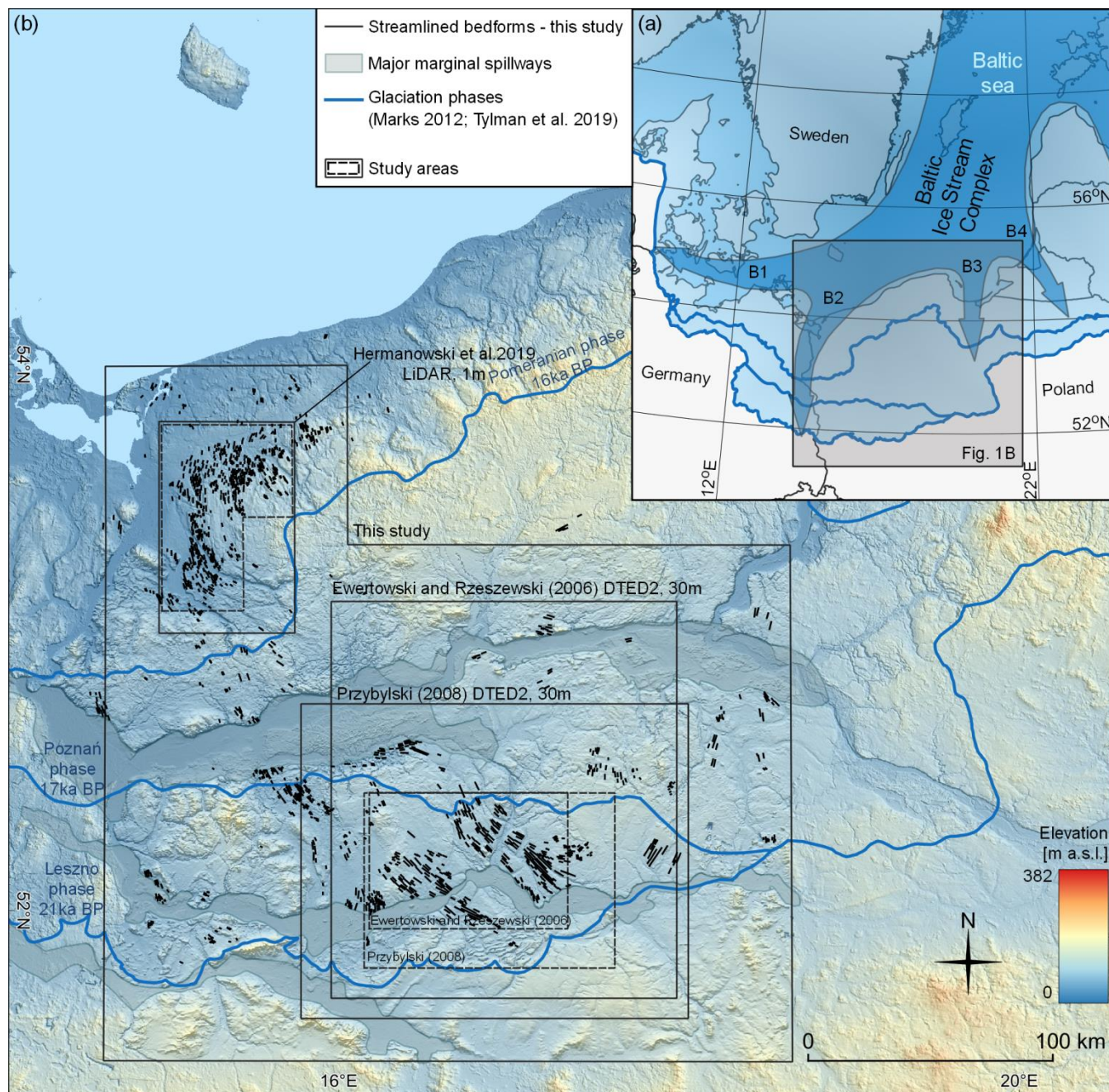


**Figure 1:** (a) An overview of Baltic Ice Stream Complex, southern sector of the SIS with B1-B4 ice streams after Punkari (1997). (b) Study area including the extent of previous studies that have mapped streamlined bedforms and major marginal spillways. Dashed lines indicate a bounding envelope for streamlined bedforms detected during previous studies. The difference between bounding envelopes for studies with overlapping areas indicate that a DEM pixel size of 30 m produces ambiguity in the detection of streamlined bedforms near the local LGM.

90



### 3 Methods

We used high-resolution LIDAR point cloud data (GUGiK, 2017) to generate a DEM with a 0.4 m ground sampling distance (GSD) across an area of about 250 x 300 km. Raw LIDAR data were distributed in square tiles of 1 x 1 km, with an average  
95 survey point density between 4 and 6 pts/m<sup>2</sup>. Several highly urbanised complexes were covered by 0.5 x 0.5 km tiles with a density of 15-20 pts/m. The terrain coordinate system was EPSG:2180 (Table 1). The original dataset comprised about 65 000 raw data files and therefore required scripting to optimise the DEM generation process.

**Table 1: Details of EPSG:2180 coordinates system**

Parameter	Value
EPSG code	2180
Reference ellipsoid	GRS80
Projection type	Transverse Mercator
Prime meridian	19°E (y <sub>0</sub> = 500 000 m)
Standard parallel	0° (x <sub>0</sub> = -5 300 000,00 m)
Scale factor at prime meridian	0.9993
Unit	m

The original data files were filtered leaving only points classified as a part of ground surface. Since the bottleneck for pre-  
100 processing was disk storage transfer, each file was compressed using the LASzip algorithm (Isenburg, 2013) reducing the storage size of the files by 7-25%. Both operations were performed as a single step using the las2las procedure of LAStools library (Hug et al., 2004). The DEM was generated using the PDAL library (PDAL Contributors, 2018), assigning terrain height values based on Shepard's inverse distance weighting algorithm (Shepard, 1968), with an empirically adjusted radius of 4 m based on their density.

105 Further raster processing steps were performed using the GDAL library (Warmerdam, 2008). Merging (*gdal\_merge*) resulted in more than 200 16x16 km tiles. Hillshade models were dynamically generated in Quantum GIS (*qgis.org*) using multidirectional sun azimuths from 0 to 90° and from 270 to 360° with increments of 45°; a sun altitude of 45°, and variable vertical exaggeration factor from 15 to 45 (estimated empirically for each subregion to emphasize small landforms). Such an approach aimed to improve landform recognition (Smith and Clark, 2005), enabling more accurate detection of landforms of  
110 different orientation compared to investigations limited to only two orthogonal directions.

A second raster dataset was produced by de-trending the DEM data. Mean elevation was derived using a bilinear resampling algorithm across a 2 x 2 km window (*gdal\_translate*) and this was subtracted from the original terrain elevation (*gdal\_calc*). The de-trended images enabled glacial landforms on slopes to be better distinguished. Such an approach was not valid in the



vicinity of meltwater valleys where steep slopes resulted in underestimation of the mean value used in the subtraction and  
115 thus disturbed the results.

The mapping process was based on semi-transparent hillshade images superimposed on the DEM and de-trended model. The  
DEM, de-trended and hillshaded raster files were enhanced with pyramids (*gdaladdo*) to facilitate map browsing over such a  
large area. Three operators independently mapped the study area to minimise the risk of landform misinterpretation. The  
resultant dataset is a minimalistic version, comprising only landforms recognized and verified by all three operators.  
120 Additional validation of uncertain bedforms was performed using raw point clouds and ground-truthing.

We classified the glacial landforms into eight groups: (i) streamlined bedforms, comprising Mega-Scale Glacial Lineations  
(MSGs) and drumlins; (ii) major and (iii) minor marginal features both including, moraine ridges, abrupt margins, edges of  
ice-contact fans, with major marginal landforms marking terminal positions of ice streams or the main recessional phases,  
and minor marginal landforms comprising sequences of moraine ridges, delicate isolated crests and abrupt margins  
125 delineating subsequent positions of the receding ice streams; (iv) ribbed moraines, (v) tunnel valleys (vi) eskers; (vii)  
geometrical ridge networks and (viii) hill-hole pairs.

The coordinate system of the result dataset was based on the coordinate system of the original point cloud dataset (Table 1).  
The projection zone width of 10°, designed to comply with the territory of Poland, resulted in the scale factor at the prime  
meridian producing length distortions of up to 70 cm/km at the E border of the study area. In the worst-case scenario,  
130 measurement of streamlined bedforms at the borders of the study area and oriented longitudinally resulted in an elongation  
error of 0.07%. Taking into consideration overall uncertainty of the dataset (see Section 5), such error is irrelevant for  
analyses focused on the distribution and morphological characteristics of glacial landforms (Clark et al., 2009; Spagnolo et  
al., 2014; Ely et al., 2016) or tying numerical modeling with their morphology (Jamieson et al., 2016).

#### 4 Results of mapping – A GIS dataset of glacial features

135 In this study, we have produced a GIS dataset of glacial features, focused on landforms that provide information on ice  
dynamics. The dataset is available here: <http://doi.org/10.5281/zenodo.4570570> (Szuman et al., 2021a) and contains 5461  
features in Geopackage format (*geopackage.org*). The glacial geomorphology map prepared from the dataset is presented in  
Fig. 2 and available via the Supplementary Data. A full morphological description and interpretation of the landforms is  
presented elsewhere (Szuman et al., 2021b); here, we outline the general characteristics of landforms included in the dataset  
140 (Fig. 3, 4).

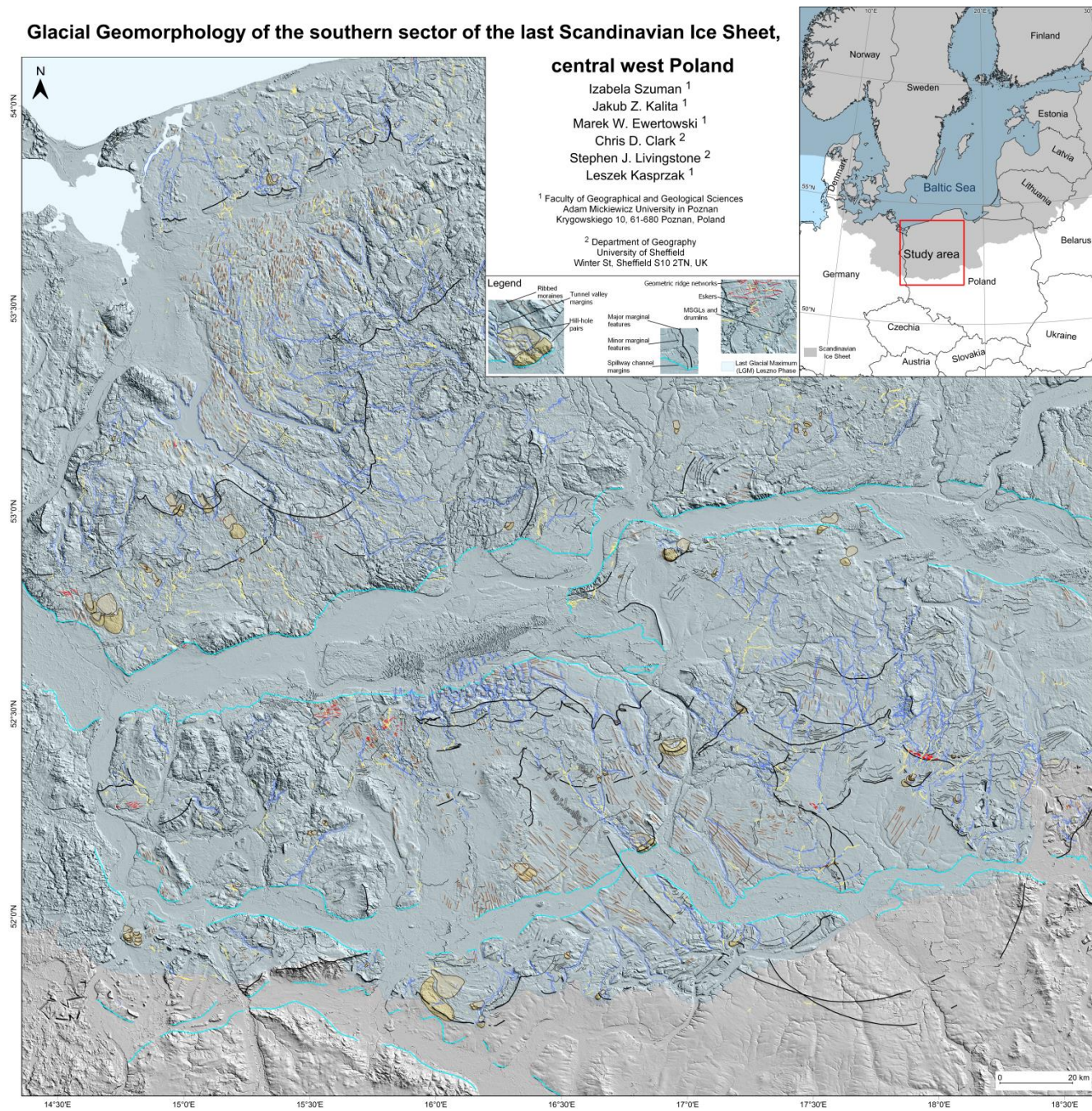
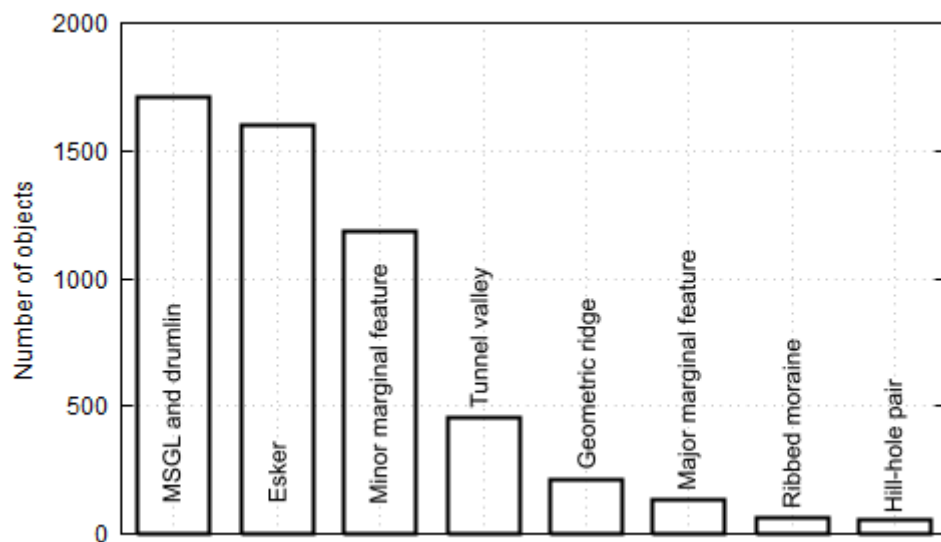


**Figure 2: Glacial geomorphology of the southern sector of the last Scandinavian Ice Sheet, central west Poland. This is designed to be viewed at a scale of 1:500000 and will need downloading from supplementary material (Fig. S1 at <http://doi.org/10.5281/zenodo.4570570>) to identify all features (see Szuman et al., 2021a).**



145

Figure 3: Number of objects for each of the mapped landform groups.

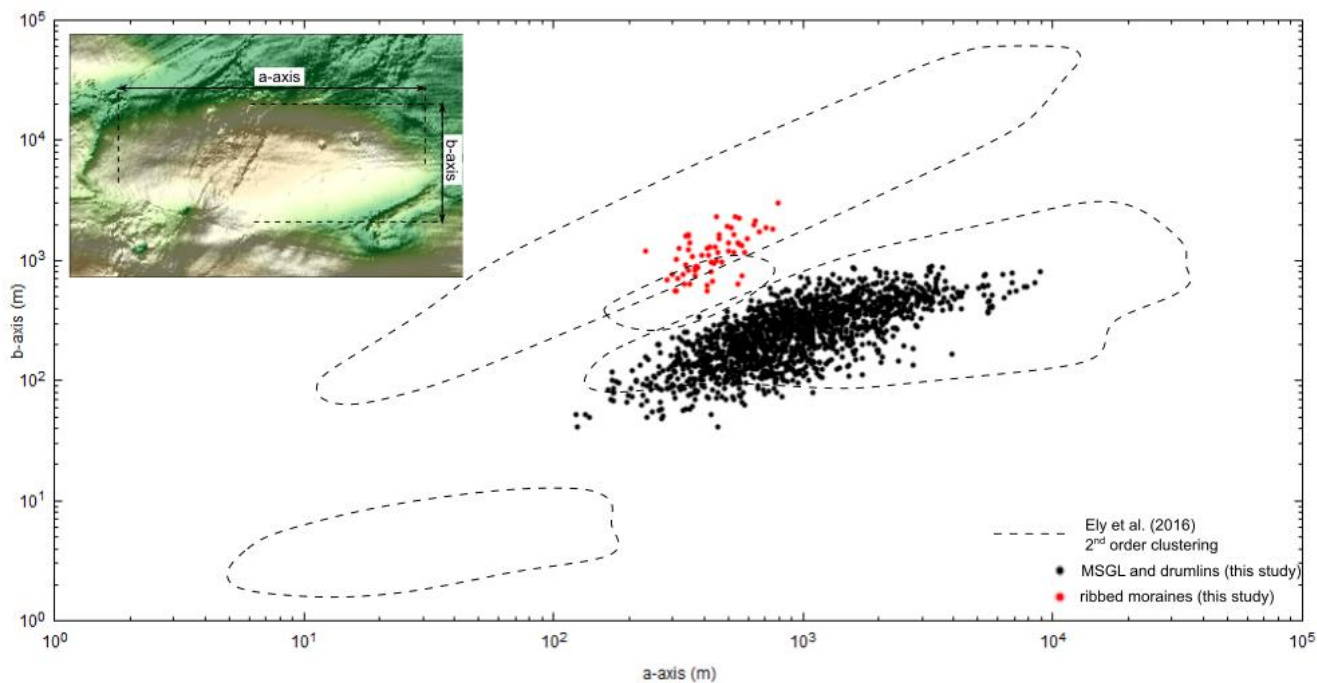


Figure 4: Dimensions of mapped MSGL, drumlins and ribbed moraines on top of subglacial bedforms continuum presented by Ely et al. (2016) as an ellipsoidal geomorphological clusters.



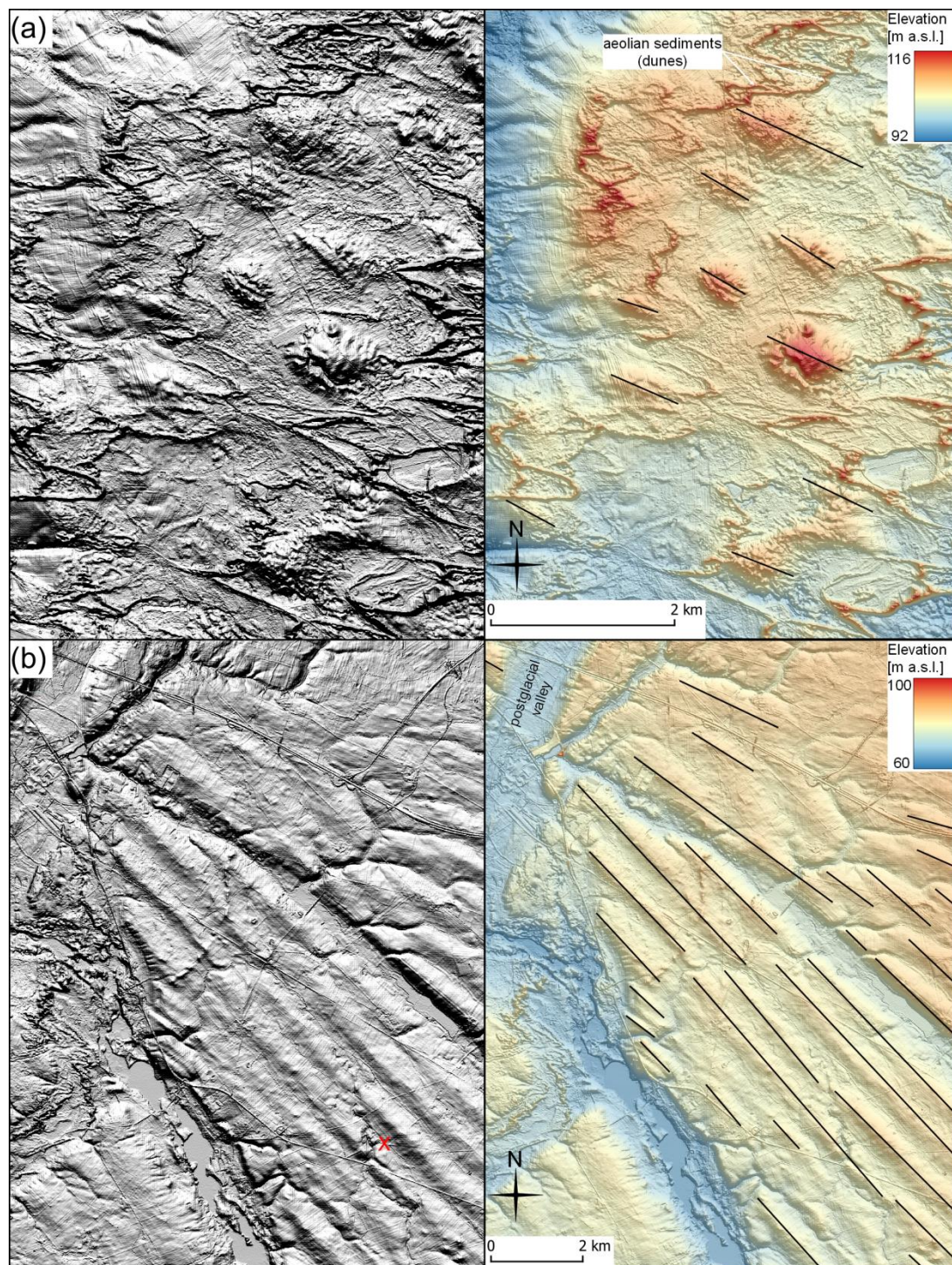
#### 150 **4.1 Streamlined bedforms: MSGs and drumlins**

MSGs have a linear topographic expression that can be sustained for over 40 km in length (Clark, 1993), with typical lengths of between about 1 and 9 km, widths between 90 and 720 m, and spacing between 140 and 960 m (Spagnolo et al., 2014). MSGs are one of the key geomorphological criteria for identifying former ice streams (Stokes and Clark, 2001), often occur with less elongated drumlins and have a convergent pattern of flow in the ice stream onset zone and fan-shaped  
155 divergence pattern near the margin (Stokes and Clark, 1999). A typical drumlin is a smooth, streamlined hill resembling the bowl of a spoon aligned longitudinally to ice movement direction (cf. Clark et al., 2009). Drumlin lengths are typically between 100 and 1000 m with widths typically three times smaller (Clark et al., 2009). Even though drumlins and MSGs are often treated separately, taking their shape and size, they form a morphological continuum of subglacial lineations (Stokes et al., 2013; Ely et al., 2016) and therefore possibly share a similar origin (see also Stokes, 2018).

160 We mapped MSGs and drumlins along their crests (Fig. 5, cf. Spagnolo et al., 2014; Ely et al., 2016). In the study area we identified 1712 MSGs and drumlins with lengths of up to 10 km, widths between 50 and 800 m, and elongation ratios up to 1:60 (Fig. 3). They are mostly found in two areas: Stargard Drumlin Field in the NE of the study area, and the central part of the area between the Poznań and Leszno Phases (Fig. 1). Due to their association with high ice flow velocity (Jamieson et al., 2016) they were one of the key elements in the identification of 17 palaeo-ice streams (see Szuman et al., 2021b).

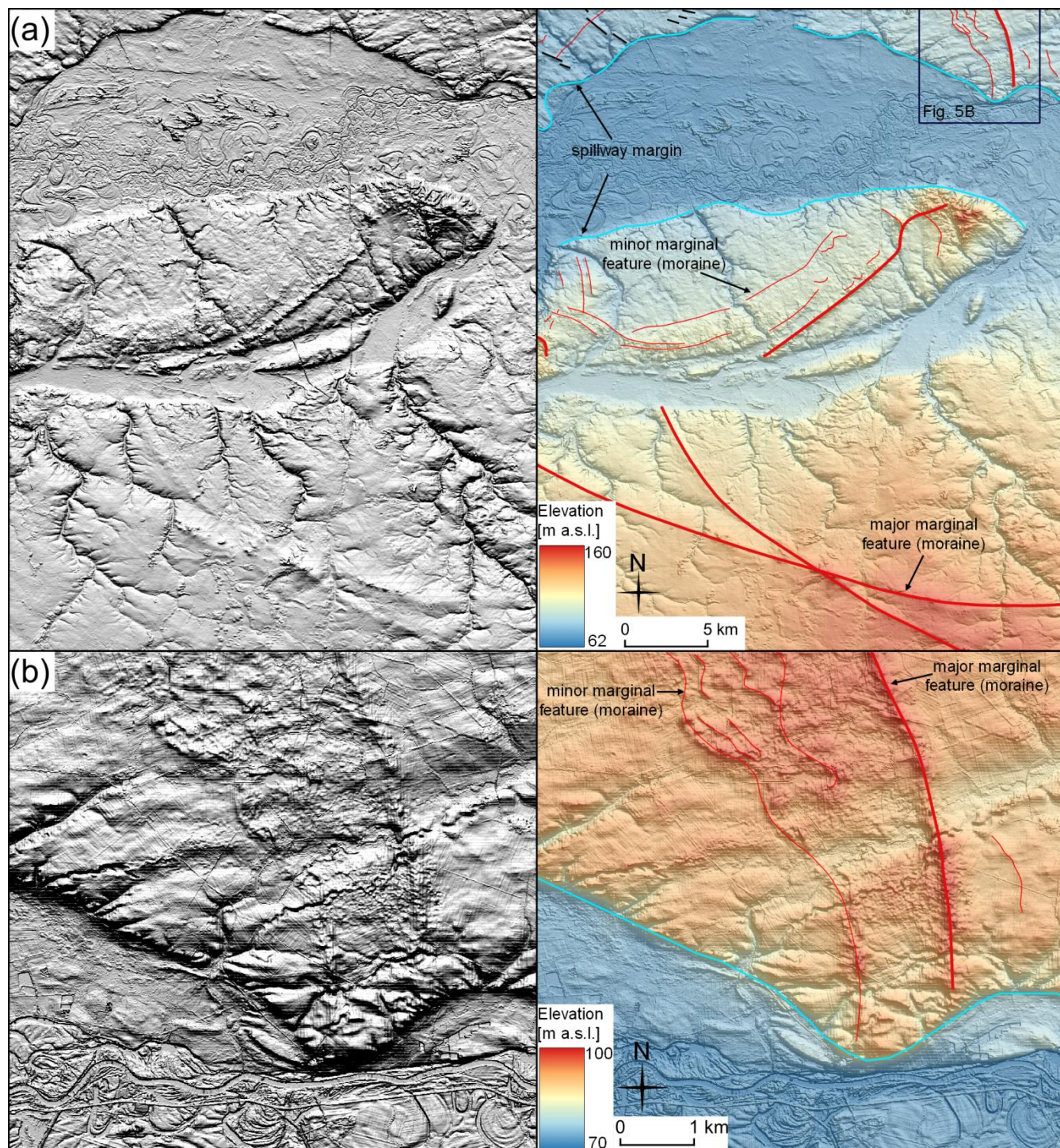
#### 165 **4.2 Major and minor marginal features**

The marginal position of ice streams was identified from: (i) moraine ridges, (ii) abrupt margins, and (iii) edges of ice-contact fans. Moraine ridges are accumulations of glacial material formed at the ice margin during a recession, standstill or re-advance (e.g. Barr and Lovell, 2014). In our study, an abrupt margin relates to lateral or terminal margins of the former ice streams marked by distinct change in topography, i.e., a switch from streamlined terrain to ribbed moraine (e.g. Vérité et al., 2020; Szuman et al., 2021b), or a steep-sloped topographic step, formed at an ice contact-face or ice stream lateral margin  
170 (Patton et al., 2016b; Alley et al., 2019), without any distinctive moraine chains. An ice-contact fan is a cone of glacial and glaci-fluvial sediments formed at the ice margin (Benn and Evans, 2010). They are asymmetrical, comprising a gentle distal slope and steep proximal slope with a steep edge. Marginal landforms were classified as major or minor. Major marginal landforms are typically associated with the terminal moraines of ice streams, abrupt margins, main stillstands, or distinct lateral moraines (Fig. 6A). In the study area, the remnants of terminal moraines constitute either clear or vestigial arcuate ridges sporadically exceeding 10 m in amplitude and 2 km in width. Minor marginal landforms represent recessional and push moraines, and cupola hills with amplitudes up to several meters and widths typically below 400 m (Fig. 6B). Limited sedimentological investigations prohibited a more detailed genetic classification.



180

**Figure 5:** Plain hillshade model (left) and DEM superimposed on hillshade model (right) with mapped (a) drumlins and (b) MSGLs as polylines along their crests. Where discontinuities in landforms (e.g., indicated with red X in Fig. 5B - hillshade) were interpreted as arising from postglacial activity from the action of water erosion, aeolian processes, or anthropogenic activity, the shape of the original landform was mapped.



185

**Figure 6: Examples of marginal features as a hillshade model (left) and DEM superimposed on hillshade model (right). (a) Cross-cutting of major marginal moraines. (b) Close-up on minor marginal moraines. Notice the prominent ice-marginal spillway disturbing the continuity of other glacial forms.**



### 4.3 Ribbed moraines

- 190 Ribbed moraines are parallel-spaced ridges, oriented transverse to the ice flow direction (Dunlop and Clark, 2006). They constitute sets formed subglacially in association with reduced ice flow velocities and typically found up-ice from drumlins and MSGs (Ely et al., 2016), at ice streams shear margins (Vérité et al., 2020; Szuman et al., 2021b) or superimposed on streamlined bedforms (Stokes et al., 2008). In the study area, ribbed moraines form three elongated ribbons parallel to inferred ice flow direction located at the sides of areas interpreted as being occupied by ice streams (Szuman et al., 2021b).
- 195 The ribbed moraine ridges in the study area are up to about 400 m wide and 2 km long, with amplitudes of about 2 m (Fig. 7) and occupy areas up to 20 km long.

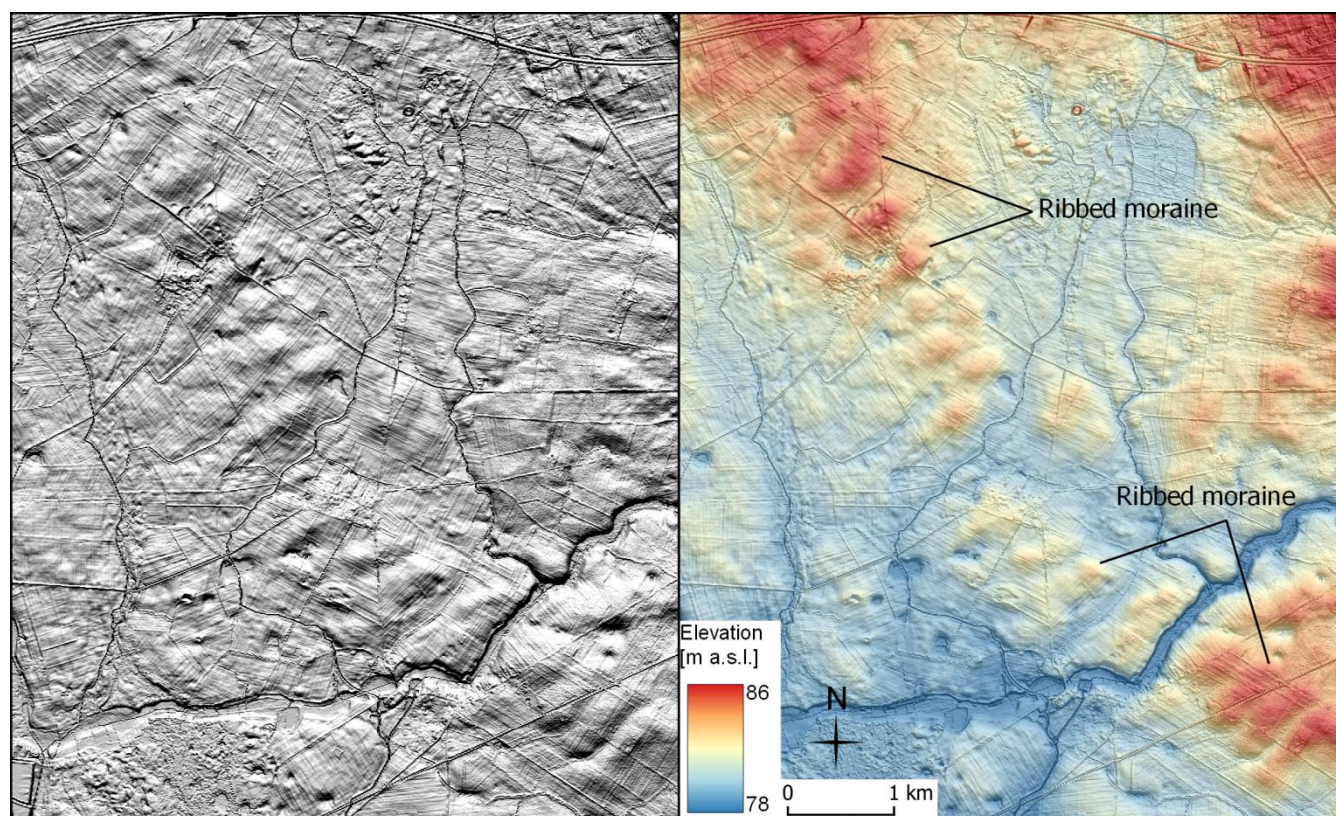


Figure 7: Examples of ribbed moraine as plain hillshade model (left) and DEM superimposed on hillshade model (right).

### 4.4 Hill-hole pairs

- 200 A hill-hole pair (Fig. 8A) comprises an ice-thrusted hill, concave up-glacier, located a short distance downstream from a depression of similar size and shape (Bluemle and Clayton, 1984; Benn and Evans, 2010). Hill-hole pairs are interpreted to form at the thin margin of advancing glaciers by plucking of large blocks of material from their frozen bed (Moran et al. 1980). Basal freezing induces compressive subglacial stresses leading to glaciotectonism (Moran et al., 1980; Rise et al., 2016). We identified about 50 of such features with relief of up to 50 m and typical widths between 1 and 4 km up to 15 km.



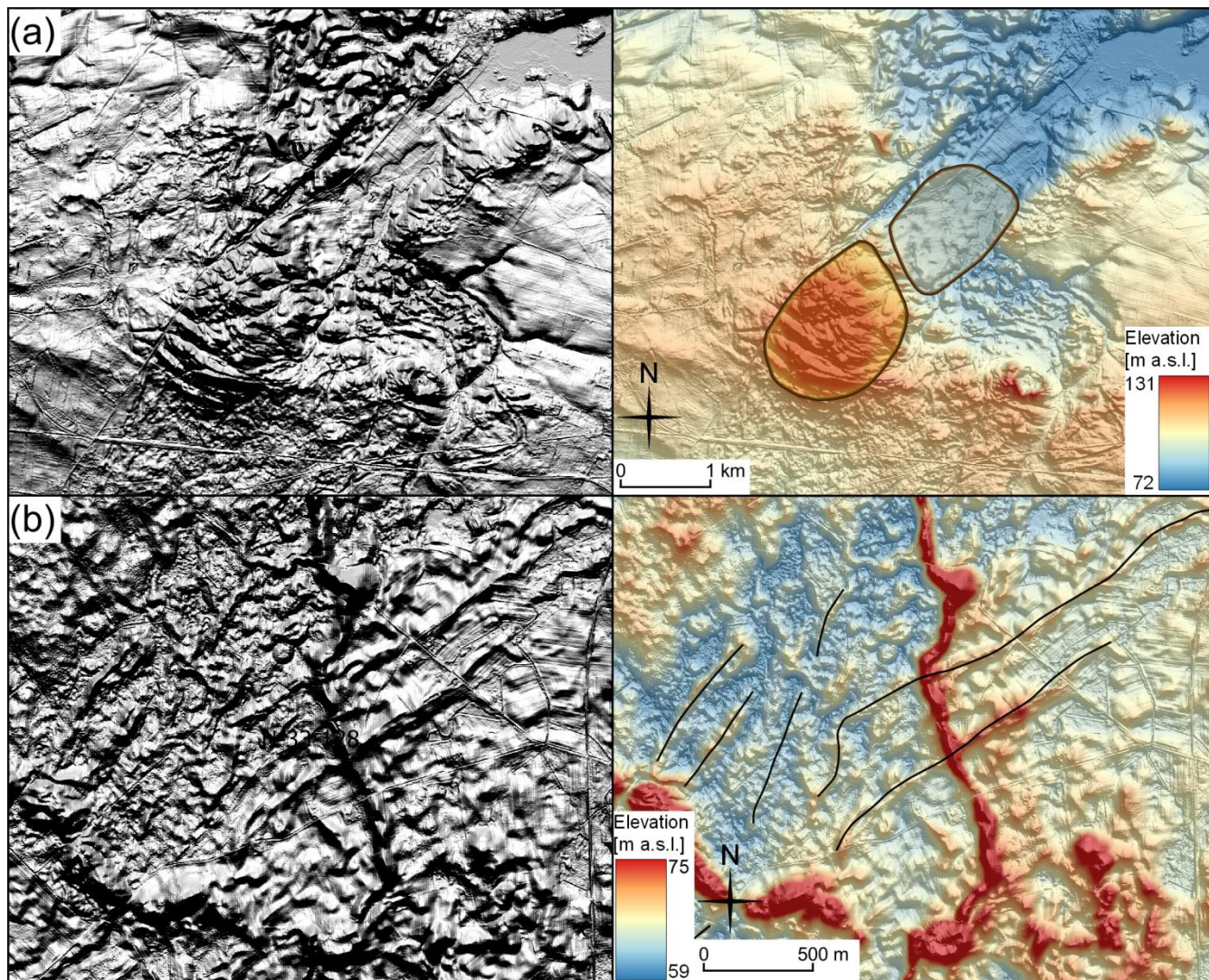
205 They are typically associated with ice stream margins and often occur near the terminal parts of tunnel valleys (see Livingstone and Clark, 2016).

#### 4.5 Geometrical ridge network

The term geometrical ridge network is a non-genetic description of glacial landforms with an organised ridge pattern, either sub-parallel to each other (e.g. Rea and Evans, 2011) or cross-cutting at acute angles (e.g. Bennett et al., 1996), typically  
210 inherited from ice structures. They are thought to originate from: (i) squeezing of subglacial sediments into basal crevasses (Evans and Rea, 1999; Evans et al., 2008; Evans et al., 2014); (ii) sediments melting-out from thrust planes and longitudinal foliation (Bennett et al., 1996; Glasser et al., 1998); or (iii) infilling of supraglacial crevasses with debris. For the features to be preserved, they require ice flow cessation and stagnation (e.g. Evans et al., 2016). Their preservation potential is low, so they are rare in glaciated areas comparing to other landforms. We identified 214 linear ridges with lengths up to 3 km,  
215 amplitudes up to 10 m and spacing up to 1 km developed transverse to the ice flow direction. In the study area, they can be found superimposed on MSGs (Fig. 8B).

#### 4.6 Eskers

Eskers are sinusoidal ridges, usually orientated parallel to the ice flow, and composed of glacial sands and gravels (Benn and Evans, 2010) deposited typically by meltwater in subglacial channels, and less often in englacial and supraglacial  
220 channels (Hebrand and Åmark, 1989). They are often interpreted to form time-transgressively, close to a retreating margin (Kleman and Borgström, 1996; Storrar et al., 2014a, b; Livingstone et al., 2020). In our study, round-, sharp- and flat-crested eskers (see Perkins et al., 2016) are present. They constitute either single or multiple-crested forms, sporadically forming dendritic networks of ridges (e.g., Fig. 9). The eskers in the study area are relatively short, rarely exceeding lengths of 10 km in comparison to eskers described from the bed of the Laurentide Ice Sheet (Storrar et al., 2014b). They are especially  
225 abundant in the northern part of the study area, related to the Pomeranian Phase (Fig. 2), but occur less frequently near the LGM margin.



230 Figure 8: Examples of (a) hill-hole-pairs and (b) geometrical ridge network, as plain hillshade model (left) and DEM superimposed on hillshade model (right).

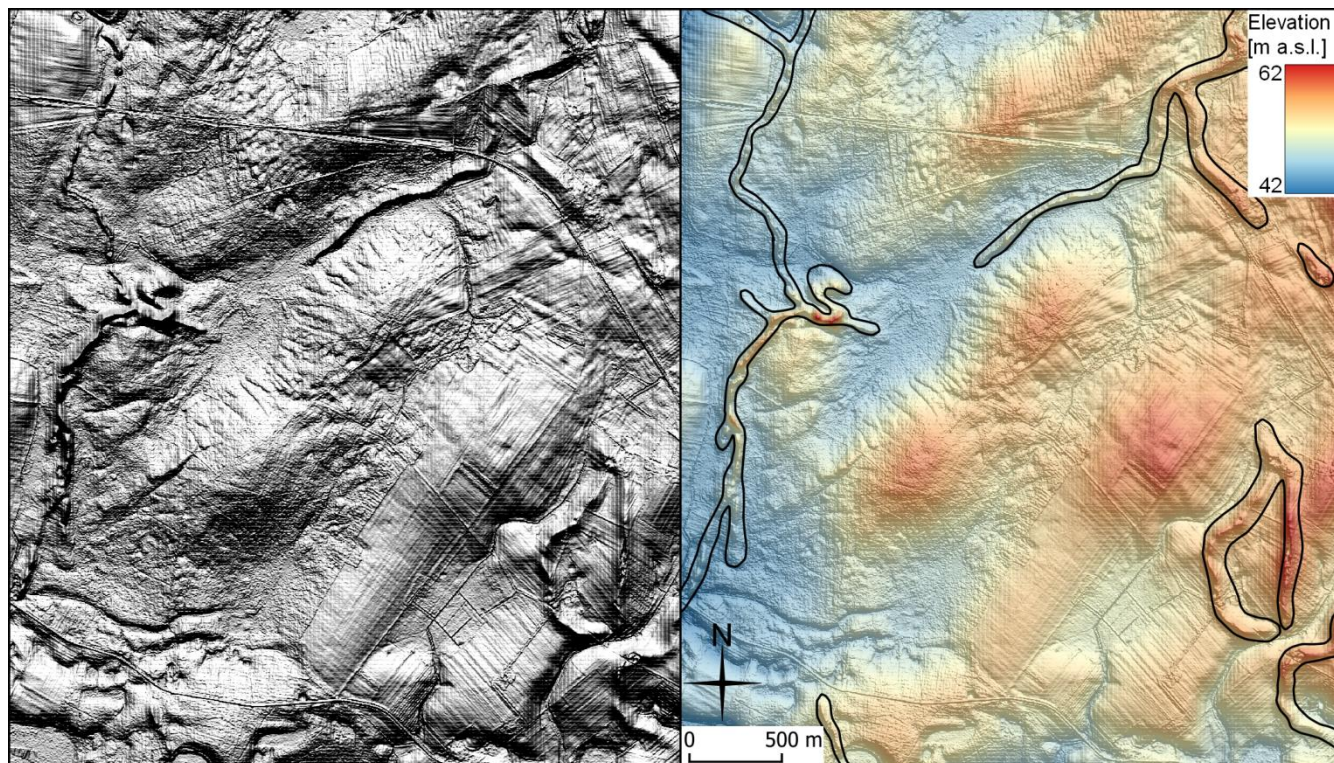
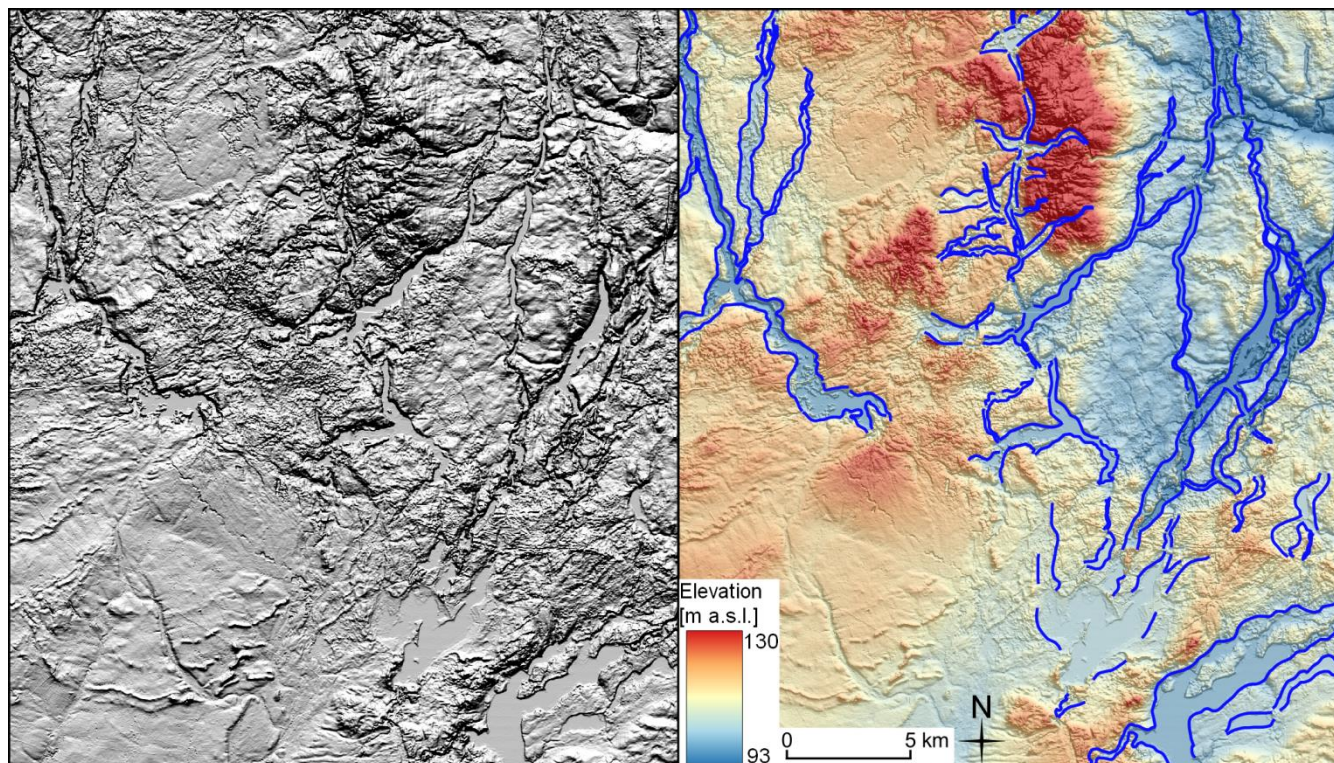


**Figure 9:** Examples of eskers, along a drumlin field, as plain hillshade model (left) and DEM superimposed on hillshade model (right).

#### 4.7 Tunnel valleys

235 Tunnel valleys are formed subglacially due to meltwater erosion as a result of either outburst floods or by a gradual/steady  
state mechanism (Ó Cofaigh, 1996; Livingstone and Clark, 2016). The subglacial water flow is driven by gradients in  
hydraulic potential (function of the bed and ice elevation) (Shreve, 1972), resulting in orientations typically parallel to  
glacier flow (Kehew et al., 2012). Tunnel valleys are often associated with eskers, terminate near former ice margins and  
have undulating long profiles (Kehew et al., 2012). We identified 456 tunnel valleys in the study area (Fig. 10). The main  
240 tunnel valleys have a quasi-regular spacing of about 5 and 10 km across the margins of the main glaciation phases  
(Figs 1, 2), with most of them occurring across the Poznań and Pomeranian margins. They often exceed 20 km in length,  
which is high (cf. Ottesen et al., 2020). However, their typical width below 2 km is conformant with counterparts of the  
Scandinavian Ice Sheet (cf. Jørgensen and Sandersen, 2006).

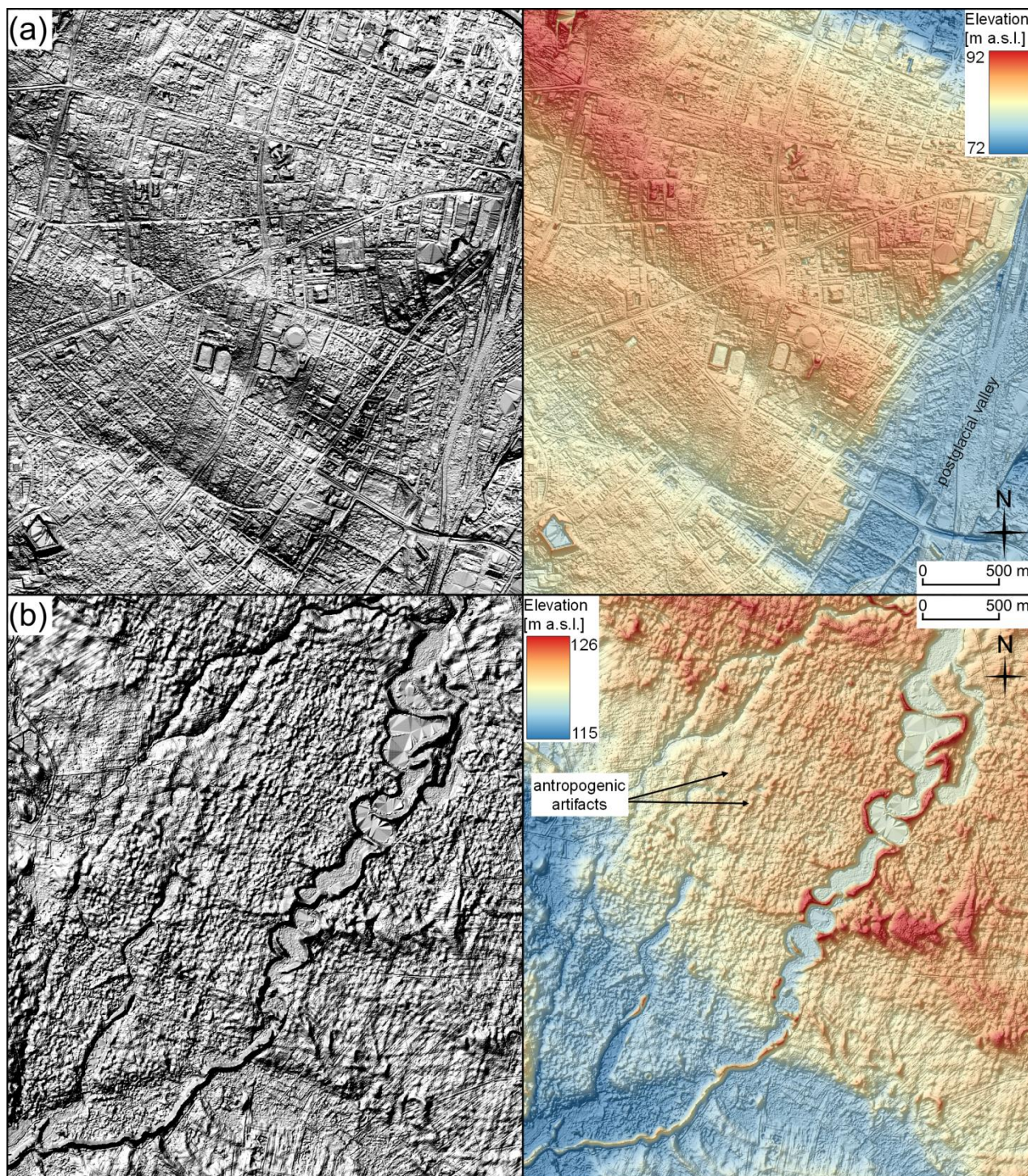


245 **Figure 10: Examples of tunnel valleys as plain hillshade model (left) and DEM superimposed on hillshade model (right).**

### 5 Limitations and uncertainty of the dataset

As noted by Spagnolo et al. (2014), increasing the scale of the DEM enabled more accurate recognition of low relief and fragmented forms. It also improved the identification of the bounding break of slopes of streamlined bedforms, enabling more accurate geomorphological parametrization (Clark et al., 2009). As shown by Napieralski and Nalepa (2010),  
250 decreasing the grid cell size from 10 to 1 m does not improve the identification of drumlins. However, it does improve the identification and geomorphological interpretation of more delicate forms, such as geometrical ridge networks, small eskers, minor moraines and narrow MSGs (Figs 1, 12). As the resolution of the DEM model applied in this study (grid cell size of 0.4 m) far exceeds the dimensions of the indicated forms, no additional uncertainty due to model quality is introduced (cf. Hättestrand and Clark, 2006). The uncertainty of the resultant data lies in the degradation of the forms and misinterpretation  
255 during the mapping process. To minimize misinterpretations, we only added a feature to the final dataset if it was indicated by three independent operators.

Subglacial forms in some parts of the study area are degraded by large-scale, human activity (forestry, farming, urbanization; cf. Przybylski, 2008; Spagnolo et al., 2016), which obscures the glacial geomorphological record (Fig. 11A). The scale difference between the degrading effect and the original form is the main factor determining the degradation potential.



260

**Figure 11. (a) Highly urbanized area on top of MSGLs interrupted by postglacial valley. Notice that the scale difference of the imprint for both groups results in small degradation potential; (b) There is an impression of delicate streamlined bedforms, which are in fact of anthropogenic origin. Ground truthing showed that they are forestry artefacts.**



265 Delicate streamlined bedforms, such as some MSGs with expected widths and spacing below 100 m reach the scale of  
anthropogenic terrain modifications, potentially leading to single cases of misinterpretation. For example, field verification  
showed that some landforms initially interpreted as MSGs, were in fact old forestry roads (Fig. 11B). Many landforms are  
partly or fully covered by aeolian sediments (dunes; Fig. 5A) that hampered landform interpretation. The continuity of many  
of the mapped bedforms in our dataset is broken by water erosion (Fig. 5B). In particular, two prominent E-W oriented  
spillways cross inferred paths of streamlined bedform fields (Figs 1, 6). The classification of ridges along large hummocky  
270 areas was also problematic as delicate landforms have been partly buried (Fig. 2; cf. Hättestrand and Clark, 2006).

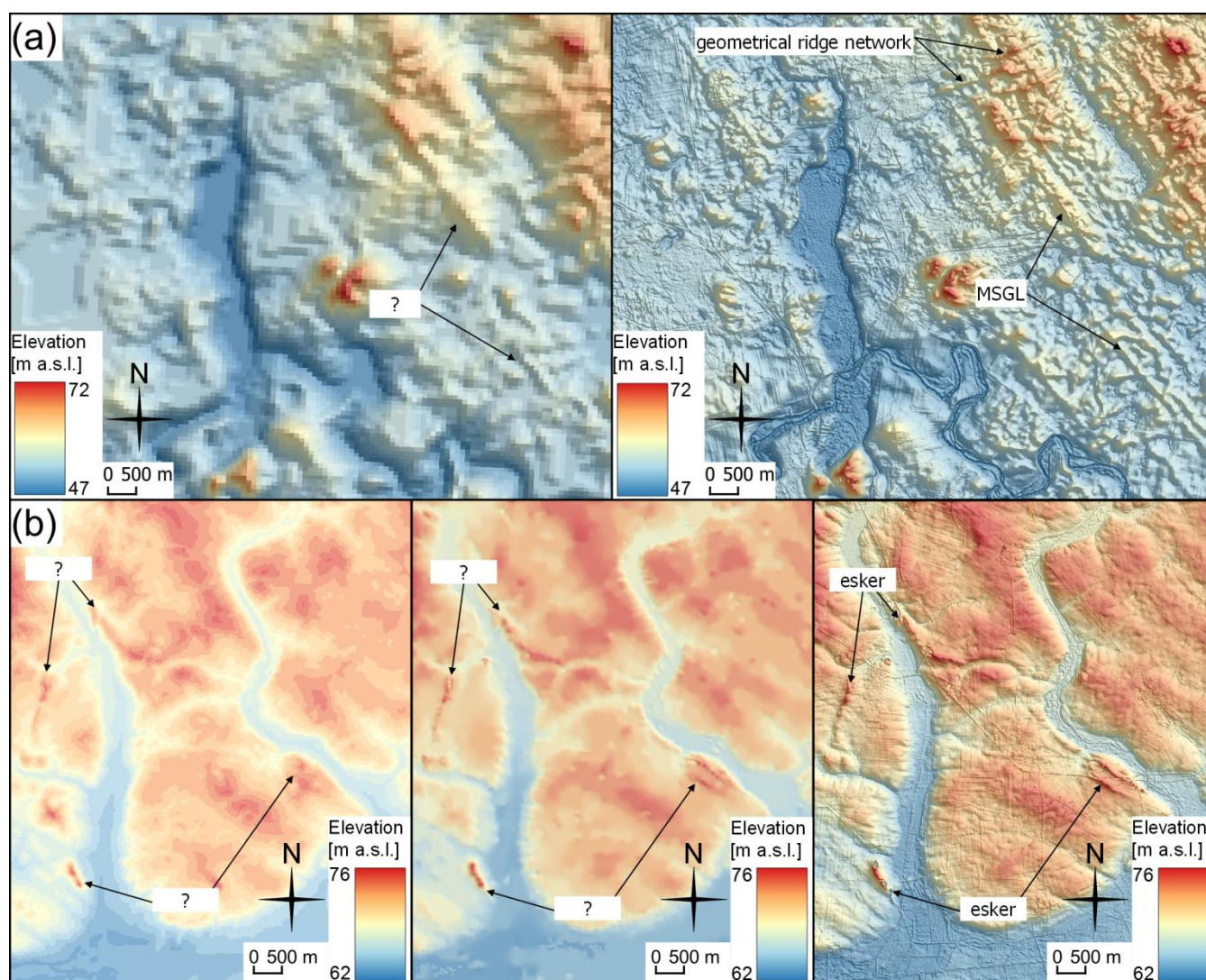


**Figure 12.** (a) Examples of delicate MSGs and geometric ridge networks on DTED2 30 m (left) and LiDAR-based 0.4 m DEM; (b) Examples of eskers near the LGM margin using DTED2 30 m (left), 1:10,000 contour-derived 5 m (middle) and LiDAR-based 0.4 m DEM. Notice how the higher-resolution model improves landform identification and interpretation.



275 Since the interpretation of post-glacially degraded forms is challenging, they are often excluded from analyses (e.g. Spagnolo et al., 2014). In our dataset, the original shape of the forms was approximated and extrapolated where possible based on a comparison between terrain profiles and profiles expected for a particular form. Taking into consideration the general level of degradation such an approach increases the number of complete objects in the resultant dataset.

## 6 Significance of the data set

280 Compared to previous mapping efforts based on low-resolution data (30-100 m GSD), we use a 0.4 m Lidar DEM, that allowed for much more detailed mapping. This has resulted in the identification of completely new sets of landforms. We have mapped 5461 glacial landforms or landform parts in the southern sector of the last Scandinavian Ice Sheet. Despite some degradation of landforms, the study area represents one of the few regions in onshore Europe with well-preserved assemblages of MSGs (Spagnolo et al., 2016). These data constitute a valuable source for reconstructing ice dynamics and  
285 constraining modelling of the southern sector of the last Scandinavian Ice Sheet, which drained the large Baltic Ice Stream Complex and was rich in terrestrially-terminating ice streams (see Szuman et al., 2021b). In addition, the southernmost sector of the Scandinavian Ice Sheet responded sensitively to climate changes (Kozarski, 1962; Patton et al., 2016a; cf. Stroeve et al., 2016), and therefore provides an analogue for modelling the future response of the Greenland and Antarctic Ice Sheets. The produced dataset is useful for researchers working on ice stream dynamics, the response of ice to climatic  
290 changes and subglacial landform formation. These data allow comparison between subglacial landforms between localities, including both formerly glaciated and modern glaciated areas occupied by ice streams.

## 7 Data availability

The data set can be accessed at <http://doi.org/10.5281/zenodo.4570570> (Szuman et al., 2021a).

## Authors contribution

295 IS, MWE, LK conceived the project. IS led the project and wrote the initial version of the manuscript, subsequently improved by the contribution of all co-authors. IS, JZK, MWE, mapped the landforms. All co-authors contributed to the interpretation of problematic areas.

## Funding and acknowledgements

This work was supported by the Polish National Science Centre (NCN) under Grant [2015/17/D/ST10/01975]. Chris Clark  
300 and Stephen Livingstone were supported by the PalGlac project funded from the European Research Council (ERC) under the European Union's Horizon 2020 research and innovation programme (Grant agreement No. 787263)



## References

- Alley, R. B., Cuffey, K. M., and Zoet, L. K.: Glacial erosion: status and outlook, *Annals of Glaciology*, 60, 1-13, <https://doi.org/10.1017/aog.2019.38>, 2019.
- 305 Assmann, P., and Dammer, B.: Geologische Karte von Preussen und benachbarten Bundesstaaten, Blatt Gross Gay, 1:25 000, Königliche Preussische Geologische Landesanstalt, Berlin, 1916.
- Bamber, J. L., Vaughan, D. G., and Joughin, I.: Widespread Complex Flow in the Interior of the Antarctic Ice Sheet, *Science*, 287, 1248, <https://doi.org/10.1126/science.287.5456.1248>, 2000.
- Bamber, J. L., and Dawson, G. J.: Complex evolving patterns of mass loss from Antarctica's largest glacier, *Nature Geoscience*, 13, 127-131, <https://doi.org/10.1038/s41561-019-0527-z>, 2020.
- 310 Barr, I. D., and Lovell, H.: A review of topographic controls on moraine distribution, *Geomorphology*, 226, 44-64, <https://doi.org/10.1016/j.geomorph.2014.07.030>, 2014.
- Bartkowski, T.: Próba kartograficznego ujęcia geomorfologii okolic Buka, Szamotuł i Skoków, *Prace Komisji Geograficzno-Geologicznej* 3, 1-50, 1962 (in Polish).
- 315 Bartkowski, T.: Deglacjacja arealna – zasadniczy typdeglacji na obszarach niżowych, *Prace Komisji Geograficzno-Geologicznej*, 70, 338-347, 1963 (in Polish).
- Bartkowski, T.: O formach rozcięcia marginalnego i niektórych formach strefy marginalnej na Nizinie Wielkopolskiej (cz. II), *Badania Fizjograficzne nad Polską Zachodnią*, 13, 7-76, 1964 (in Polish).
- 320 Bartkowski, T.: O formach strefy marginalnej na Nizinie Wielkopolskiej, *Prace Komisji Geograficzno-Geologicznej*, 7, 1-260, 1967 (in Polish).
- Bartkowski, T.: Kemy na obszarze Niziny Wielkopolskiej a deglacjacja (in Polish), *Badania Fizjograficzne nad Polską Zachodnią*, 21, 7-77, 1968.
- Bartkowski, T.: Deglacjacja strefowa deglacjacją normalną na obszarach niżowych, na wybranych przykładach z Polski Zachodniej, *Badania Fizjograficzne nad Polską Zachodnią*, 23A, 7-34, 1969 (in Polish).
- 325 Bartkowski, T.: Strefa marginalna stadiału pomorskiego w aspekcie deglacjacji strefowej (na wybranych przykładach z Pojezierzy Drawskiego i Miastkowskiego na Pomorzu), *Badania Fizjograficzne nad Polską Zachodnią*, 26A, 7-60, 1972 (in Polish).
- Benn, D. I., and Evans, D. J. A.: *Glaciers and glaciation*, Hodder Education, London, 2010.
- Bennett, M. R., Hambrey, M. J., Huddart, D., and Ghienne, J. F.: The formation of a geometrical ridge network by the surge-type glacier Kongsvegen, Svalbard, *Journal of Quaternary Science*, 11, 437-449, [https://doi.org/10.1002/\(SICI\)1099-1417\(199611/12\)11:6<437::AID-JQS269>3.0.CO;2-J](https://doi.org/10.1002/(SICI)1099-1417(199611/12)11:6<437::AID-JQS269>3.0.CO;2-J), 1996.
- 330 Berendt, G., and Keilhack, K.: Endmoränen in der Provinz Posen, *Jb. D. Kön. Preuss. Geol. Landesanst.*, 13, 235-237, 1894 (in German).
- Bluemle, J. P., and Clayton, L. E. E.: Large-scale glacial thrusting and related processes in North Dakota, *Boreas*, 13, 279-299, <https://doi.org/10.1111/j.1502-3885.1984.tb01124.x>, 1984.
- Boulton, G. S., Dongelmans, P., Punkari, M., and Broadgate, M.: Palaeoglaciology of an ice sheet through a glacial cycle: the European ice sheet through the Weichselian, *Quaternary Science Reviews*, 20, 591-625, [https://doi.org/10.1016/S0277-3791\(00\)00160-8](https://doi.org/10.1016/S0277-3791(00)00160-8), 2001.
- 335 Boulton, G. S., Dongelmans, P., Punkari, M., and Broadgate, M.: Evidence of European ice sheet fluctuation during the last glacial cycle, in: *Developments in Quaternary Sciences*, edited by: Ehlers, J., and Gibbard, P. L., Elsevier, 441-460, 2004.



- 340 Chandler, B. M. P., Lovell, H., Boston, C. M., Lukas, S., Barr, I. D., Benediktsson, Í. Ö., Benn, D. I., Clark, C. D., Darvill, C. M., Evans, D. J. A., Ewertowski, M. W., Loibl, D., Margold, M., Otto, J.-C., Roberts, D. H., Stokes, C. R., Storrar, R. D., and Stroeven, A. P.: Glacial geomorphological mapping: A review of approaches and frameworks for best practice, *Earth-Science Reviews*, 185, 806-846, <https://doi.org/10.1016/j.earscirev.2018.07.015>, 2018.
- Clark, C. D.: Mega-scale glacial lineations and cross-cutting ice-flow landforms, *Earth Surface Processes and Landforms*, 18, 1-29, [10.1002/esp.3290180102](https://doi.org/10.1002/esp.3290180102), 1993.
- 345 Clark, C. D.: Reconstructing the evolutionary dynamics of former ice sheets using multi-temporal evidence, remote sensing and GIS, *Quaternary Science Reviews*, 16, 1067-1092, [https://doi.org/10.1016/S0277-3791\(97\)00037-1](https://doi.org/10.1016/S0277-3791(97)00037-1), 1997.
- Clark, C. D., Spagnolo, M., Hughs, A. L. C., Greenwood, S. L., Stokes, C. R., Dunlop, P., and Ng, F.: A re-examination of drumlin morphology; width, length, height, elongation, and asymmetry, *INQUA VII International Drumlin Symposium*, 2009,
- Dunlop, P., and Clark, C. D.: The morphological characteristics of ribbed moraine, *Quaternary Science Reviews*, 25, 1668-1691, <https://doi.org/10.1016/j.quascirev.2006.01.002>, 2006.
- 350 Ely, J. C., Clark, C. D., Spagnolo, M., Stokes, C. R., Greenwood, S. L., Hughes, A. L. C., Dunlop, P., and Hess, D.: Do subglacial bedforms comprise a size and shape continuum?, *Geomorphology*, 257, 108-119, <https://doi.org/10.1016/j.geomorph.2016.01.001>, 2016.
- Ely, J. C., Clark, C. D., Hindmarsh, R. C. A., Hughes, A. L. C., Greenwood, S. L., Bradley, S. L., Gasson, E., Gregoire, L., Gandy, N., Stokes, C. R., and Small, D.: Recent progress on combining geomorphological and geochronological data with ice sheet modelling, demonstrated using the last British–Irish Ice Sheet, *Journal of Quaternary Science*, n/a, <https://doi.org/10.1002/jqs.3098>, 2019a.
- 355 Ely, J. C., Clark, C. D., Small, D., and Hindmarsh, R. C. A.: ATAT 1.1, the Automated Timing Accordance Tool for comparing ice-sheet model output with geochronological data, *Geosci. Model Dev.*, 12, 933-953, <https://doi.org/10.5194/gmd-12-933-2019>, 2019b.
- Evans, D. J. A., and Rea, B. R.: Geomorphology and sedimentology of surging glaciers: a land-systems approach, *Annals of Glaciology*, 28, 75-82, <https://doi.org/10.3189/172756499781821823>, 1999.
- 360 Evans, D. J. A., Clark, C. D., and Rea, B. R.: Landform and sediment imprints of fast glacier flow in the southwest Laurentide Ice Sheet, *Journal of Quaternary Science*, 23, 249-272, <https://doi.org/10.1002/jqs.1141>, 2008.
- Evans, D. J. A., Young, N. J. P., and Ó Cofaigh, C.: Glacial geomorphology of terrestrial-terminating fast flow lobes/ice stream margins in the southwest Laurentide Ice Sheet, *Geomorphology*, 204, 86-113, <https://doi.org/10.1016/j.geomorph.2013.07.031>, 2014.
- Evans, D. J. A., Storrar, R. D., and Rea, B. R.: Crevasse-squeeze ridge corridors: Diagnostic features of late-stage palaeo-ice stream activity, *Geomorphology*, 258, 40-50, <https://doi.org/10.1016/j.geomorph.2016.01.017>, 2016.
- 365 Ewertowski, M., and Rzeszewski, M.: Using DEM to recognize possible minor stays of Vistulian (Weichselian) ice-sheet margin in the Wielkopolska Lowland, *Quaestiones Geographicae*, 25A, 7-21, 2006.
- Galon, R.: Morphology of the Noteć-Warta (or Toruń-Everswalde) ice marginal streamway, *Wydawnictwa Geologiczne*, Warsaw, 1961.
- Glasser, N. F., Hambrey, M. J., Crawford, K. R., Bennett, M. R., and Huddart, D.: The structural glaciology of Kongsvegen, Svalbard, and its role in landform genesis, *Journal of Glaciology*, 44, 136-148, <http://doi.org/10.3189/S0022143000002422>, 1998.
- 370 Hättestrand, C., and Clark, C. D.: The glacial geomorphology of Kola Peninsula and adjacent areas in the Murmansk Region, Russia, *Journal of Maps*, 2, 30-42, <http://doi.org/10.4113/jom.2006.41>, 2006.
- Hebrand, M., and Åmark, M.: Esker formation and glacier dynamics in eastern Skane and adjacent areas, southern Sweden, *Boreas*, 18, 67-81, <https://doi.org/10.1111/j.1502-3885.1989.tb00372.x>, 1989.



- 375 Hermanowski, P., Piotrowski, J. A., and Szuman, I.: An erosional origin for drumlins of NW Poland, *Earth Surface Processes and Landforms*, 0, <http://doi.org/10.1002/esp.4630>, 2019.
- Houmark-Nielsen, M.: Extent, age and dynamics of Marine Isotope Stage 3 glaciations in the southwestern Baltic Basin, *Boreas*, 39, 343-359, <http://doi.org/10.1111/j.1502-3885.2009.00136.x>, 2010.
- Hug, C., Krzystek, P., and Fuchs, W.: Advanced LiDAR data processing with LasTools, ISPRS Congress, Istanbul, 2004,
- 380 Hughes, A. L. C., Gyllencreutz, R., Lohne, Ø. S., Mangerud, J., and Svendsen, J. I.: The last Eurasian ice sheets – a chronological database and time-slice reconstruction, DATED-1, *Boreas*, 45, 1-45, <http://doi.org/10.1111/bor.12142>, 2016.
- Hughes, T.: Modeling ice sheets from the bottom up, *Quaternary Science Reviews*, 28, 1831-1849, <https://doi.org/10.1016/j.quascirev.2009.06.004>, 2009.
- Isenburg, M.: LASzip: lossless compression of Lidar data, *Photogrammetric Engineering & Remote Sensing*, 79, 209-217, <http://doi.org/10.14358/PERS.79.2.209>, 2013.
- 385 Jamieson, S. S. R., Stokes, C. R., Livingstone, S. J., Vieli, A., Ó Cofaigh, C., Hillenbrand, C.-D., and Spagnolo, M.: Subglacial processes on an Antarctic ice stream bed. 2: Can modelled ice dynamics explain the morphology of mega-scale glacial lineations?, *Journal of Glaciology*, 62, 285-298, <http://doi.org/10.1017/jog.2016.19>, 2016.
- Jørgensen, F., and Sandersen, P. B. E.: Buried and open tunnel valleys in Denmark—erosion beneath multiple ice sheets, *Quaternary Science Reviews*, 25, 1339-1363, <https://doi.org/10.1016/j.quascirev.2005.11.006>, 2006.
- 390 Joughin, I., and Tulaczyk, S.: Positive Mass Balance of the Ross Ice Streams, West Antarctica, *Science*, 295, 476, <http://doi.org/10.1126/science.1066875>, 2002.
- Kalm, V.: Ice-flow pattern and extent of the last Scandinavian Ice Sheet southeast of the Baltic Sea, *Quaternary Science Reviews*, 44, 51-59, <https://doi.org/10.1016/j.quascirev.2010.01.019>, 2012.
- 395 Karczewski, A.: Morfologia, struktura i tekstura moreny dennej na obszarze Polski zachodniej, *Prace Komisji Geograficzno-Geologicznej*, 4, 1-111, 1963 (in Polish).
- Karczewski, A.: Zmienność litologiczna i strukturalna kemow Pomorza Zachodniego a zagadnienie ich klasyfikacji, *Prace Komisji Geograficzno-Geologicznej*, 11, 1-57, 1971 (in Polish).
- Karczewski, A.: Morphometric features of drumlins in western Pomerania, *Quaestiones Geographicae*, 3, 35-42, 1976.
- 400 Karczewski, A., Kozarski, S., and Rotnicki, K.: Przeglądowa Mapa Geomorfologiczna Polski, arkusz Poznań, 1: 500 000, Instytut Geografii i Przestrzennego Zagospodarowania PAN, Kraków, 1980 (in Polish).
- Kehew, A. E., Piotrowski, J. A., and Jørgensen, F.: Tunnel valleys: Concepts and controversies — A review, *Earth-Science Reviews*, 113, 33-58, <https://doi.org/10.1016/j.earscirev.2012.02.002>, 2012.
- Keilhack, K.: *Abhandlungen der Königlich Preussischen Geologischen Landesanstalt : neue Folge 1897 H. 26, Im Vertrieb der Simon Schropp'schen Hof - Landkartenhandlung, Berlin, 1897 (in German).*
- 405 King, E. C., Hindmarsh, R. C. A., and Stokes, C. R.: Formation of mega-scale glacial lineations observed beneath a West Antarctic ice stream, *Nature Geoscience*, 2, 585, <http://doi.org/10.1038/ngeo581>, 2009.
- Kjær, K. H., Houmark-Nielsen, M., and Richardt, N.: Ice-flow patterns and dispersal of erratics at the southwestern margin of the last Scandinavian Ice Sheet: signature of palaeo-ice streams, *Boreas*, 32, 130-148, <http://doi.org/10.1111/j.1502-3885.2003.tb01434.x>, 2003.



- 410 Kleman, J., and Borgström, I.: Reconstruction of palaeo-ice sheets: the use of geomorphological data, *Earth Surface Processes and Landforms*, 21, 893-909, [http://doi.org/10.1002/\(sici\)1096-9837\(199610\)21:10<893::Aid-esp620>3.0.Co;2-u](http://doi.org/10.1002/(sici)1096-9837(199610)21:10<893::Aid-esp620>3.0.Co;2-u), 1996.
- Kleman, J., Hättestrand, C., Borgström, I., and Stroeven, A.: Fennoscandian palaeoglaciology reconstructed using a glacial geological inversion model, *Journal of Glaciology*, 43, 283-299, <http://doi.org/10.3189/S0022143000003233>, 1997.
- Kleman, J., Stroeven, A. P., and Lundqvist, J.: Patterns of Quaternary ice sheet erosion and deposition in Fennoscandia and a theoretical framework for explanation, *Geomorphology*, 97, 73-90, <https://doi.org/10.1016/j.geomorph.2007.02.049>, 2008.
- 415 Kleman, J., Jansson, K., De Angelis, H., Stroeven, A. P., Hättestrand, C., Alm, G., and Glasser, N.: North American Ice Sheet build-up during the last glacial cycle, 115–21kyr, *Quaternary Science Reviews*, 29, 2036-2051, <https://doi.org/10.1016/j.quascirev.2010.04.021>, 2010.
- Korn, J.: Die Mittel-Posensche Endmorane und die damit verbundenen Oser, *Jb. d. Kgl. Preuss. Geol. Landesanst.*, 33, 478-518, 1912 (in German).
- 420 Kozarski, S.: O genezie chodzieskiej moreny czołowej, *Badania Fizjograficzne nad Polską Zachodnią*, 5, 45-72, 1959 (in Polish).
- Kozarski, S.: Recesja ostatniego lądolodu z północnej części Wysoczyzny Gnieźnieńskiej a kształtowanie się Pradoliny Noteci-Warty, *Państwowe Wydawnictwo Naukowe, Poznań*, 154 pp., 1962 (in Polish).
- Kozarski, S.: Lithologie und Genese der Endmoränen im Gebiet der skandinavischen Vereisungen, *Schriftenreihe für Geologische Wissenschaften*, 9, 179-200, 1978 (in German).
- 425 Kozarski, S.: Deglacjacja polnocno-zachodniej Polski: warunki środowiska i transformacja geosystemu [ok.20 KA - 10 KA BP], *Dokumentacja Geograficzna*, 1, 1-82, 1995 (in Polish).
- Krygowski, B.: Przeglądowa mapa geologiczna Polski, arkusz C 2, 1: 300 000, *Państwowy Instytut Geologiczny, Poznań*, 1947 (in Polish).
- 430 Krygowski, B.: Mapa Geomorfologiczna Niziny Wielkopolsko-Kujawskiej (in Polish), *Adam Mickiewicz University, Poznań*, 1963 (in Polish).
- Liedtke, H.: Die nordischen Vereisungen in Mitteleuropa, *Zentralausschuß für Dt. Landeskunde, Trier* 1981 (in German).
- Livingstone, S. J., and Clark, C. D.: Morphological properties of tunnel valleys of the southern sector of the Laurentide Ice Sheet and implications for their formation, *Earth Surf. Dynam.*, 4, 567-589, <http://doi.org/10.5194/esurf-4-567-2016>, 2016.
- 435 Livingstone, S. J., Lewington, E. L. M., Clark, C. D., Storrar, R. D., Sole, A. J., McMartin, I., Dewald, N., and Ng, F.: A quasi-annual record of time-transgressive esker formation: implications for ice-sheet reconstruction and subglacial hydrology, *The Cryosphere*, 14, 1989-2004, <http://doi.org/10.5194/tc-14-1989-2020>, 2020.
- Lukas, S.: Morphostratigraphic principles in glacier reconstruction -a perspective from the British Younger Dryas, *Progress in Physical Geography: Earth and Environment*, 30, 719-736, <http://doi.org/10.1177/0309133306071955>, 2006.
- 440 MacAyeal, D. R.: Binge/purge oscillations of the Laurentide Ice Sheet as a cause of the North Atlantic's Heinrich events, *Paleoceanography*, 8, 775-784, <https://doi.org/10.1029/93PA02200>, 1993.
- Moran, S. R., Clayton, L., Hooke, R. L., Fenton, M. M., and Andriashek, L. D.: Glacier-Bed Landforms of The Prairie Region of North America, *Journal of Glaciology*, 25, 457-476, <http://doi.org/10.3189/S0022143000015306>, 1980.
- 445 Napieralski, J., Li, Y., and Harbor, J.: Comparing predicted and observed spatial boundaries of geologic phenomena: Automated Proximity and Conformity Analysis applied to ice sheet reconstructions, *Computers & Geosciences*, 32, 124-134, <https://doi.org/10.1016/j.cageo.2005.05.011>, 2006.



- Napieralski, J., Harbor, J., and Li, Y.: Glacial geomorphology and geographic information systems, *Earth-Science Reviews*, 85, 1-22, <https://doi.org/10.1016/j.earscirev.2007.06.003>, 2007.
- Napieralski, J., and Nalepa, N.: The application of control charts to determine the effect of grid cell size on landform morphometry, *Computers & Geosciences*, 36, 222-230, <https://doi.org/10.1016/j.cageo.2009.06.003>, 2010.
- 450 Ottesen, D., Stewart, M., Brønner, M., and Batchelor, C. L.: Tunnel valleys of the central and northern North Sea (56°N to 62°N): Distribution and characteristics, *Marine Geology*, 425, 106199, <https://doi.org/10.1016/j.margeo.2020.106199>, 2020.
- Ó Cofaigh, C.: Tunnel valley genesis, *Progress in Physical Geography: Earth and Environment*, 20, 1-19, <http://doi.org/10.1177/030913339602000101>, 1996.
- 455 Ó Cofaigh, C., Dowdeswell, J. A., Evans, J., and Larter, R. D.: Geological constraints on Antarctic palaeo-ice-stream retreat, *Earth Surface Processes and Landforms*, 33, 513-525, <http://doi.org/10.1002/esp.1669>, 2008.
- Patton, H., Hubbard, A., Andreassen, K., Winsborrow, M., and Stroeven, A. P.: The build-up, configuration, and dynamical sensitivity of the Eurasian ice-sheet complex to Late Weichselian climatic and oceanic forcing, *Quaternary Science Reviews*, 153, 97-121, <https://doi.org/10.1016/j.quascirev.2016.10.009>, 2016a.
- 460 Patton, H., Swift, D. A., Clark, C. D., Livingstone, S. J., and Cook, S. J.: Distribution and characteristics of overdeepenings beneath the Greenland and Antarctic ice sheets: Implications for overdeepening origin and evolution, *Quaternary Science Reviews*, 148, 128-145, <https://doi.org/10.1016/j.quascirev.2016.07.012>, 2016b.
- Patton, H., Hubbard, A., Andreassen, K., Auriac, A., Whitehouse, P. L., Stroeven, A. P., Shackleton, C., Winsborrow, M., Heyman, J., and Hall, A. M.: Deglaciation of the Eurasian ice sheet complex, *Quaternary Science Reviews*, 169, 148-172, <https://doi.org/10.1016/j.quascirev.2017.05.019>, 2017.
- 465 PDAL Contributors: PDAL Point Data Abstraction Library, <http://doi.org/10.5281/zenodo.2556738>, 2018.
- Perkins, A. J., Brennand, T. A., and Burke, M. J.: Towards a morphogenetic classification of eskers: Implications for modelling ice sheet hydrology, *Quaternary Science Reviews*, 134, 19-38, <https://doi.org/10.1016/j.quascirev.2015.12.015>, 2016.
- Przybylski, B.: Geomorphic traces of a Weichselian ice stream in the Wielkopolska Lowland, western Poland, *Boreas*, 37, 286-296, <http://doi.org/10.1111/j.1502-3885.2007.00023.x>, 2008.
- 470 Punkari, M.: Glacial and glaciofluvial deposits in the interlobate areas of the Scandinavian ice sheet, *Quaternary Science Reviews*, 16, 741-753, [https://doi.org/10.1016/S0277-3791\(97\)00020-6](https://doi.org/10.1016/S0277-3791(97)00020-6), 1997.
- Rahmstorf, S.: Ocean circulation and climate during the past 120,000 years, *Nature*, 419, 207-214, <http://doi.org/10.1038/nature01090>, 2002.
- 475 Rea, B. R., and Evans, D. J. A.: An assessment of surge-induced crevassing and the formation of crevasse squeeze ridges, *Journal of Geophysical Research: Earth Surface*, 116, <http://doi.org/10.1029/2011Jf001970>, 2011.
- Retzlaff, R., and Bentley, C. R.: Timing of stagnation of Ice Stream C, West Antarctica, from short-pulse radar studies of buried surface crevasses, *Journal of Glaciology*, 39, 553-561, <http://doi.org/10.3189/S0022143000016440>, 1993.
- 480 Rignot, E., Mouginot, J., Scheuchl, B., van den Broeke, M., van Wessem, M. J., and Morlighem, M.: Four decades of Antarctic Ice Sheet mass balance from 1979–2017, *Proceedings of the National Academy of Sciences*, 116, 1095, <http://doi.org/10.1073/pnas.1812883116>, 2019.
- Rise, L., Bellec, V. K., Ottesen, D., Bøe, R., and Thorsnes, T.: Hill–hole pairs on the Norwegian continental shelf, *Geological Society, London, Memoirs*, 46, 203, <http://doi.org/10.1144/M46.42>, 2016.



- Rotnicki, K., and Borówka, R. K.: Osady górnego plenivistulianu w dolinie dolnej Prosną pod Macewem a wiek maksymalnego zasięgu ostatniego zlodowacenia podczas fazy leszczyńskiej, *Badania Fizjograficzne nad Polską Zachodnią*, 40A, 5-20, 1989 (in Polish).
- 485 Rotnicki, K., and Borówka, R. K.: Stratigraphy, palaeogeography and dating of the North Polish Stage, in: *Changes of the Polish Coastal Zone*, edited by: Rotnicki, K., Adam Mickiewicz University, Poznań, 1994.
- Shepard, D.: A two-dimensional interpolation function for irregularly-spaced data, *Proceedings of the 1968 23rd ACM national conference*, 1968.
- Shreve, R. L.: Movement of Water in Glaciers, *Journal of Glaciology*, 11, 205-214, <https://doi.org/10.3189/S002214300002219X>, 1972.
- 490 Smith, M. J., and Clark, C. D.: Methods for the visualization of digital elevation models for landform mapping, *Earth Surface Processes and Landforms*, 30, 885-900, <https://doi.org/10.1002/esp.1210>, 2005.
- Spagnolo, M., Clark, C. D., Ely, J. C., Stokes, C. R., Anderson, J. B., Andreassen, K., Graham, A. G. C., and King, E. C.: Size, shape and spatial arrangement of mega-scale glacial lineations from a large and diverse dataset, *Earth Surface Processes and Landforms*, 39, 1432-1448, <https://doi.org/10.1002/esp.3532>, 2014.
- 495 Spagnolo, M., Phillips, E., Piotrowski, J. A., Rea, B. R., Clark, C. D., Stokes, C. R., Carr, S. J., Ely, J. C., Ribolini, A., Wysota, W., and Szuman, I.: Ice stream motion facilitated by a shallow-deforming and accreting bed, *Nature Communications*, 7, <https://doi.org/10.1038/ncomms10723>, 2016.
- Stankowski, W.: Geneza Wału Lwówecko-Rakoniewickiego oraz jego obrzeżenia w świetle badań geomorfologicznych i sedimentologicznych, 8, 1-94, 1968 (in Polish).
- 500 Stokes, C. R., and Clark, C. D.: Geomorphological criteria for identifying Pleistocene ice streams, *Annals of Glaciology*, 28, 67-74, [10.3189/172756499781821625](https://doi.org/10.3189/172756499781821625), 1999.
- Stokes, C. R., and Clark, C. D.: Palaeo-ice streams, *Quaternary Science Reviews*, 20, 1437-1457, [https://doi.org/10.1016/S0277-3791\(01\)00003-8](https://doi.org/10.1016/S0277-3791(01)00003-8), 2001.
- Stokes, C. R., Lian, O. B., Tulaczyk, S., and Clark, C. D.: Superimposition of ribbed moraines on a palaeo-ice-stream bed: implications for ice stream dynamics and shutdown, *Earth Surface Processes and Landforms*, 33, 593-609, <https://doi.org/10.1002/esp.1671>, 2008.
- Stokes, C. R., and Tarasov, L.: Ice streaming in the Laurentide ice sheet : a first comparison between data-calibrated numerical model output and geological evidence, *Geophysical research letters*, 37, L01501, <https://doi.org/10.1029/2009GL040990>, 2010.
- Stokes, C. R., Spagnolo, M., Clark, C. D., Ó Cofaigh, C., Lian, O. B., and Dunstone, R. B.: Formation of mega-scale glacial lineations on the Dubawnt Lake Ice Stream bed: 1. size, shape and spacing from a large remote sensing dataset, *Quaternary Science Reviews*, 77, 190-209, <https://doi.org/10.1016/j.quascirev.2013.06.003>, 2013.
- 510 Stokes, C. R., Tarasov, L., Blomdin, R., Cronin, T. M., Fisher, T. G., Gyllencreutz, R., Hättestrand, C., Heyman, J., Hindmarsh, R. C. A., Hughes, A. L. C., Jakobsson, M., Kirchner, N., Livingstone, S. J., Margold, M., Murton, J. B., Noormets, R., Peltier, W. R., Peteet, D. M., Piper, D. J. W., Preusser, F., Renssen, H., Roberts, D. H., Roche, D. M., Saint-Ange, F., Stroeven, A. P., and Teller, J. T.: On the reconstruction of palaeo-ice sheets: Recent advances and future challenges, *Quaternary Science Reviews*, 125, 15-49, <https://doi.org/10.1016/j.quascirev.2015.07.016>, 2015.
- Stokes, C. R., Margold, M., Clark, C. D., and Tarasov, L.: Ice stream activity scaled to ice sheet volume during Laurentide Ice Sheet deglaciation, *Nature*, 530, 322-326, <https://doi.org/10.1038/nature16947>, 2016.
- Stokes, C. R.: Geomorphology under ice streams: Moving from form to process, *Earth Surface Processes and Landforms*, 43, 85-123, <https://doi.org/10.1002/esp.4259>, 2018.



- 520 Storrar, R. D., Stokes, C. R., and Evans, D. J. A.: Increased channelization of subglacial drainage during deglaciation of the Laurentide Ice Sheet, *Geology*, 42, 239-242, <https://doi.org/10.1130/G35092.1>, 2014a.
- Storrar, R. D., Stokes, C. R., and Evans, D. J. A.: Morphometry and pattern of a large sample (>20,000) of Canadian eskers and implications for subglacial drainage beneath ice sheets, *Quaternary Science Reviews*, 105, 1-25, <https://doi.org/10.1016/j.quascirev.2014.09.013>, 2014b.
- 525 Stroeven, A. P., Hättstrand, C., Kleman, J., Heyman, J., Fabel, D., Fredin, O., Goodfellow, B. W., Harbor, J. M., Jansen, J. D., Olsen, L., Caffee, M. W., Fink, D., Lundqvist, J., Rosqvist, G. C., Strömberg, B., and Jansson, K. N.: Deglaciation of Fennoscandia, *Quaternary Science Reviews*, 147, 91-121, <https://doi.org/10.1016/j.quascirev.2015.09.016>, 2016.
- Szuman, I., Kalita, J. Z., Ewertowski, M., Livingstone, S. J., Clark, C. D. and Kasprzak, L.: LiDAR-based glacial geomorphological dataset, southern sector of Baltic Ice Stream Complex, last Scandinavian Ice Sheet, Poland, <http://doi.org/10.5281/zenodo.4570570>, 2021a.
- 530 Szuman, I., Kalita, J. Z., Ewertowski, M. W., Clark, C. D., and Livingstone, S. J.: Dynamics of the last Scandinavian Ice Sheet's southernmost sector revealed by the pattern of ice streams, *Boreas*, n/a, <https://doi.org/10.1111/bor.12512>, 2021b.
- Tylmann, K., Rinterknecht, V. R., Woźniak, P. P., Boulès, D., Schimmelpfennig, I., Guillou, V., and Team, A.: The Local Last Glacial Maximum of the southern Scandinavian Ice Sheet front: Cosmogenic nuclide dating of erratics in northern Poland, *Quaternary Science Reviews*, 219, 36-46, <https://doi.org/10.1016/j.quascirev.2019.07.004>, 2019.
- 535 Vérité, J., Ravier, É., Bourgeois, O., Pochat, S., Lelandais, T., Mourgues, R., Clark, C. D., Bessin, P., Peigné, D., and Atkinson, N.: Ribbed bedforms in palaeo-ice streams reveal shear margin positions, lobe shutdown and the interaction of meltwater drainage and ice velocity patterns, *The Cryosphere Discuss.*, 2020, 1-31, <https://doi.org/10.5194/tc-2020-336>, 2020 (in review).
- Warmerdam, F.: The Geospatial Data Abstraction Library, in: *Open Source Approaches in Spatial Data Handling*, edited by: Hall, G. B., and Leahy, M. G., Springer Berlin Heidelberg, Berlin, Heidelberg, 87-104, 2008.
- 540 Woldstedt, P.: *Geologisch-morphologische Übersichtskarte des Norddeutschen Vereisungsgebietes 1 : 1 500 000*, Preuss. Geol. Landesanst., Berlin, 1935 (in German).
- Wysota, W., Molewski, P., and Sokołowski, R. J.: Record of the Vistula ice lobe advances in the Late Weichselian glacial sequence in north-central Poland, *Quaternary International*, 207, 26-41, <https://doi.org/10.1016/j.quaint.2008.12.015>, 2009.